

Atomic Resolution of Topography Images Of (Graphite, Gold, N-Type Silicon Wafer and Cadmium Oxide Films) Using Stm

Faisal A. Mustafa

Laser Physics Department/College of Science for Women
Babylon University-Iraq

ABSTRACT: *Morphological surface images analyze the atomic resolution in 3-dimensions, the colored lateral images map, the graphic line, the forward and back shaded map with 3-Dimensions, for graphite, gold, n-type silicon wafer and cadmium oxide films by using scanning tunneling microscopy (STM) all are investigated. The images of surface graphite showed a regular geometrically distribution with 2.5nm hexagonal arrangement atoms about with 0.34nm level distance. But the gold surface showed a convergence atoms and great density of electrons. While the n-type Si (100) wafer refers to stacking rows and show a linear defect (dislocations) arising from inserting an extra impurities. The images clearly showed that phosphor atom located in substitutional site among silicon atoms with high nanoscale resolution. Also the mixing of oxygen molecular with cadmium and their locations appear like island. It's applied to study cadmium oxide films deposited on holder surfaces. The simulated images show the main key features of experimental observations, with ability and direct methods for imaging identical theoretically with model of tunneling quantum.*

KEYWORDS: Surface Topography, 3-Dimension Image, Metal, STM, Morphology, Semiconductor, Graphite, Gold, Silicon Wafer, Cadmium Oxide Film

INTRODUCTION

Scanning Tunneling Microscopy (STM) is a technique that can produce atomic resolution topographic images of both metal and semiconductor surfaces. STM can be a challenging technique relies on a quantum mechanical tunnel current that runs between a surface and a sharp metallic tip which are in close proximity. The fact that sets the STM apart from most other surface sensitive techniques is its ability to resolve the structure of surfaces on an atomic scale, that is atom-by-atom, and furthermore its ability to study the dynamics of surface processes. The versatile modular electronics and software are capable to provide many different data taking mode curves can provide information about the local work function and/or bound image states on metal surfaces^[1]. Its development in 1981 earned its inventors, Gerd Binnig and Heinrich Rohrer (at IBM Zürich), the Nobel Prize in Physics in 1986^{[2][3]}. For an STM, good resolution is considered to be 0.1 nm lateral resolution and 0.01 nm depth resolution^[4]. With this resolution, individual atoms within materials are routinely imaged and manipulated^[5]. The resulting tunneling current is a function of tip position, applied voltage, and the local density of states (LDOS) of the sample^[6]. Carsten Sprodowski *et al*, 2010 is used STM to study the dissociation of molecular oxygen on Ag(100) induced by inelastic electron

tunneling (IET) at 5 K^[7]. Wei-dong Dou and Han-jie Zhang, 2010 reconstructed the structures of Cu (100) surface induced by O₂ dissociative adsorption were investigated by low energy electron diffraction and SFM^[8]. Hui-li Fan *et al* 2010 observed the adsorption behavior and electronic structure of tin-phthalocyanine (SnPc) on Ag(111) surface with Sn-up and Sn-down conformations^[9]. Flemming Besenbacher, 1996 has proved STM to be a fascinating and powerful technique in the field of surface science of well characterized single crystal metal surfaces under ultra-high vacuum conditions ^[10]. Leibsle, F. M. *et al* 1997 procedure a review of surface reactions studied with (STM) which shows unprecedented insight into the mechanisms at an atomic level^[11]. Schryvers, D.*et al*, 2013 used electron tomography techniques for materials science, on different shape memory and nano structured metallic systems obtained by various three-dimensional electron imaging techniques^[12]. Frank Palmino 1990 study the structural and electronic properties of Si surfaces and metal-silicon interfaces have been carried out in our (STM) group in Marseille^[13]. Terui T.,*et al*, 2004 study porphyrin molecules on metal substrates^[14]. Zhang Yan-Feng, 2012, used chemical vapor deposition (CVD) to the large-scale synthesis of graphene on various metal substrates ^[15]. Dixon, R.1999 deposited the gold onto WO sub3 (001) at room temperature also produced bright circular maxima in STM images^[16]. Yamamoto, N., 2000, apply UHV- (STM) to the study of silver films deposited on Si (111) surfaces^[17]. Chambliss, D.D, used the STM to understand the epitaxial growth of metal films^[18].

The aim of the research is to provide a three-dimensional profile of the some conductor and semiconductor surfaces which is very useful for characterizing surface roughness, observing surface defects, coincidence theoretical tunneling quantum model, and determining the size and conformation of molecules and aggregates on the surface. The insight into small dimensions has led to a new understanding of the structure of materials, forms of life and looks into the fascinating world of the atoms. In the STM, an enormous resolution is achieved so that the atomic arrangement of metallic and semiconductor surfaces can be “probed”. Relative to other methods for achieving nano-structured silicon, Bandgap's nano-silicon processes are inexpensive, fast and controllable. The STM images of the silicon wafer and CdO structures and its arrangement of functional molecules would contribute valuable information towards creation of nano-molecular-devices.

Experimental

PHYWE compact STM system consists of control unit with mounted scan head, magnifying cover glass and measure nano software. The tip-surface distance in the STM as shown in figure 1(a) can be controlled very precisely. A bias voltage is applied and the tip is brought close to the sample by coarse sample-to-tip control, which is turned off when the tip and sample are sufficiently close. At close range, fine control of the tip in all three dimensions when near the sample is typically piezoelectric, maintaining tip-sample separation W typically in 0.4-0.7 nm range, which is the equilibrium position between attractive ($3 < W < 10 \text{ \AA}$) and repulsive ($W < 3 \text{ \AA}$) interactions^[5] as shown in figure 1(b). The components of an STM include scanning tip, piezoelectric controlled height and x,y scanner, coarse sample-to-tip control, vibration isolation system, and computer^[19]. The

The orientation of the surfaces is undetermined for all the studied samples; it must only keep the microscope and its components free of grease, and dust by using ethanol. The sample holder guide bars and the approach motor are cleaned with alcohol in the axial direction, by using a soft cloth that should be moved up-and downwards. The surface of the middle samples has to be totally very flat, and clean a like mirror, and additionally be in a non-oxidized to be conducive. The installation of some other hardware by inserting CD for the instrument. The additional needed equipment is PC/Laptop with USB port, window XP or higher with installing the measure nano software and in most cases, the autorun CD menu program opens automatically. To start measuring, the sample must be very close to the tip, to enable a tunneling current to flow. To Approach the sample without touching the tip by manual coarse approach, use the tip approach motor and automatic final approach until a given set point is reached. After a successful approach, the status light will switch to green.

The computer is connected with the supplier USB to the microscope control unit. The Z-Controller, tip properties panel, the loop gain, tunneling current, and the tip voltage will be selected to obtain imaging zoom by scanning speed (Time/line), the resolution (pixel/line) and rotation. It can zoom in and out data and switch the color map to a 3D view and measure distances between points that set in the images. The changing parameter in any panel is used to activate the parameter by clicking it with the mouse pointer.

In the Z-Controller Panel set parameters control, the tunneling current to the sample by setting the desired current will be detected when the tip is in a close distance to the sample. The value of loop grain influences the feedback loop that derives the piezo-electric device. The approach panel is used by pushing the motor units to the sample holder towards the tip and the approach bottom starts the automatic approach routine. If a sharp tip and a conducting surface are put under a low voltage ($\approx 0.1V$), a very small tunneling current ($\approx 1nA$) may flow between tip and sample. One of the three piezo crystals, the Z-piezo, can now be used in a feedback loop that keeps the tunneling constant current by changing the Z-distance appropriately.

The image size sets the edge length of the imaging area, depending on the controller, the values is from about 500nm to few nanometers and the atomic arrangements can be observed at about 10nm. The selected image will be saved with a standard file name. The chart types consisting line graph data are displayed as a plot. The points outside the range of the scanner are displayed in red. The displayed line is selected by dragging the line selection arrow in a color map or shaded map chart. Also 3-D view data is shown as 3-dimensional representation in a parallel perspective. The dual line graph both the forward and the backward data (when available) are displayed as in the "line graph". The line of the data type selected in "Signal" is black; the line of the reverse direction data is gray. The STM tip can be prepared and installed to obtain optimal measurements and atomic resolution using the pointed tweezers to bring the tip and tip holder. In measurement system a platinum-iridium tip is moved in three dimensions using piezo-crystal translators that are driven with sub-nanometer precision. It put the tip wire (Pt/Ir)

underneath the clamp on the tip holder parallel to the groove and held securely under the clamp, it should stick out about 1-2 mm beyond the tip holder.

THEORETICAL

Tunneling is a functioning concept that arises from quantum mechanics. and in the presence of a potential $U(z)$, assuming 1-dimensional case, the energy levels $\psi_n(z)$ of the electrons are given by solutions of Schrödinger's equation, the electron wave function is a traveling wave, the solution is,

$$\psi_n(z) = \psi_n(0)e^{\pm ikz} \quad (1)$$

If $E > U(z)$, which is true for a wave function inside the tip or inside the sample.^[5] Inside a barrier, $E < U(z)$ so the wave functions which satisfy this are decaying waves,

$$\psi_n(z) = \psi_n(0)e^{\pm kz} \quad (2)$$

Where K quantifies the decay of the wave inside the barrier, with the barrier in the $+z$ direction for $-\kappa$.^[4] Knowing the wave function allows one to calculate the probability density for that electron to be found at some location. Let us assume the bias is V and the barrier width is W . This probability, P , that an electron at $z=0$ (left edge of barrier) can be found at $z=W$ (right edge of barrier) is proportional to the wave function squared,^[5]

$$P \propto |\psi_n(0)|^2 e^{-2KW} \quad (3)$$

If the bias is small, we can let in the expression for κ , where ϕ , the work function, gives the minimum energy needed to bring an electron from an occupied level, the highest of which is at the Fermi level (for metals at $T=0K$), to vacuum level. Mathematically, this tunneling current is given by

$$I \propto \sum_{E_f - eV}^{E_f} |\psi_n(0)|^2 e^{-2KW} \quad (4)$$

One can sum the probability over energies between $E_f - eV$ and E_f to get the number of states available in this energy range per unit volume, thereby finding the local density of states (LDOS) near the Fermi level.^[5] The LDOS near some energy E in an interval ε is given by

$$\rho_s(z, E) = \frac{1}{\varepsilon} \sum_{E-\varepsilon}^E |\psi_n(z)|^2 \quad (5)$$

and the tunnel current at a small bias V is proportional to the LDOS near the Fermi level, which gives important information about the sample..^[5] Thus the tunneling current is given by

$$I \propto V \rho_s(0, E_f) e^{-2KW} \quad (6)$$

Published by European Centre for Research Training and Development UK (www.eajournals.org)

where $\rho_s(0, E_f)$ is the LDOS near the Fermi level of the sample at the sample surface. This current can also be expressed in terms of the LDOS near the Fermi level of the sample at the tip surface,

$$I \propto V \rho_s(W, E_f) \quad (7)$$

Now, Fermi's Golden Rule gives the rate for electron transfer across the barrier, and is written

$$w = \frac{2\pi}{\hbar} |M|^2 \delta(E_\psi - E_\chi) \quad (8)$$

where $\delta(E_\psi - E_\chi)$ restricts tunneling to occur only between electron levels with the same energy.^[51] The tunnel matrix element, given by:

$$M = \frac{\hbar^2}{2m} \int_{z=z_0} (\chi^* \frac{\partial \psi}{\partial z} - \psi \frac{\partial \chi^*}{\partial z}) dS, \quad (9)$$

is a description of the lower energy associated with the interaction of wave functions at the overlap, also called the resonance energy.^[51] Summing over all the states gives the tunneling current as

$$I = \frac{4\pi e}{\hbar} \int_{-\infty}^{+\infty} [f(E_f - eV + \varepsilon) - f(E_f + \varepsilon)] \rho_s(E_f - eV + \varepsilon) \rho_T(E_f + \varepsilon) |M|^2 d\varepsilon, \quad (10)$$

where f is the Fermi function, and are the density of states in the sample and tip, respectively^[51]. The Fermi distribution function describes the filling of electron levels at a given temperature T . The tools use to measure distances and angles. The displayed data corresponds to the lines and arrows in the color map image of the measurement. The length of the arrow in the plane of the chart. It is related to the evaluation results height, W, H are width and length according to the formula :

$$L = (W^2 + H^2)^{\frac{1}{2}} \quad (11)$$

To calculate the angle between two lines, by use a drawing them in the chart. The angle can be changed by dragging the line end point markers of the corner mark. To calculate the line roughness average from the data at points along a selected line according the following formula:

$$S_d = \frac{1}{N} \sum_{l=0}^{N-1} |z(x_l)| \quad (\text{The Valley depth, } S_v = \text{the lowest value}) \quad (12)$$

The mean value, S_m and the root mean square, S_q are given by the following equations:

$$S_m = \frac{1}{N} \sum_{l=0}^{N-1} z(x_l) \quad (\text{The Peak Height, } S_p = \text{highest value}) \quad (13)$$

$$S_d = \sqrt{\frac{1}{N} \sum_{l=0}^{N-1} (z(x_l))^2} \quad (\text{The Peak-Valley Height, } S_y = S_p - S_v) \quad (14)$$

To calculate the area roughness from the data points in a selected area by calculated width and height according the following formula:

$$S_d = \frac{1}{MN} \sum_{k=0}^{M-1} \sum_{l=0}^{N-1} |z(x_k, y_l)| \quad (\text{The Valley depth, } S_v = \textit{the lowest value}) \quad (15)$$

$$S_m = \frac{1}{MN} \sum_{k=0}^{M-1} \sum_{l=0}^{N-1} z(x_k, y_l) \quad (\text{The Peak Height, } S_p = \textit{highest value}) \quad (16)$$

$$S_d = \sqrt{\frac{1}{MN} \sum_{k=0}^{M-1} \sum_{l=0}^{N-1} (z(x_k, y_l))^2} \quad (\text{The Peak-Valley Height, } S_y = S_p - S_v) \quad (17)$$

The roughness values depend on the data filter that is applied to the chart, because these values are calculated from the filter data. The selected points are the end points of the two connected lines.

RESULTS AND DISCUSSION

Since the tunnel current is very strongly depend on the distance between the tip and the surface, we can use a feedback loop to control the distance between tip and surface to enable imaging of the surface and individual ad-atoms or ad-molecules. To achieve atomic resolution, the image size should be decreased even further, considering that one nanometer is the diameter of four and eight atoms. Atomic arrangements can normally be recognized at an image size of about 4nm. Some thermal fluctuations influence the measurements on the nanometer scale, the sample has to be scanned as fast as possible. With a good tip and properly set parameters, the atomic arrangements will be observed, includes a pattern consisting of bright, intermediate, and dark spots. It looks like a three dimensional image of balls lying next to each other. These are not the single atoms. A sharp tip and a good tunneling contact are necessary for high quality images of atomic. When a small bias V is applied in the system, only electronic states become very near to the Fermi level, within eV , are excited.^[5] When V is positive, electrons in the tip tunnel move to empty states in the sample; for a negative bias, electrons tunnel out of the occupied states in the sample into the tip.^[5] In the case of tunneling, the tip and sample wave functions overlap for ex., when it is under a bias, there is some finite probability to find the electron in the barrier region and even on the other side of the barrier. At a separation of a few atomic diameters, the tunneling current rapidly increases while the distance between the tip and the surface decreases. This rapid change of tunneling current with distance results in atomic resolution. The reduce of voltage between the tip and the surface of the sample leads to reducing the interaction between the tip and the cloud of the electrons, the best value of voltage and current are 100mV and 1nA respectively. It is observed that the best possible images get, when the distance between the scan lines

approach to atoms diameter of the surface. So to get the possible clearest image with determined dimensions, it is important to change the distance of intra-scan lines to obtain a constant dimensions of the images. The increasing image dimension leads to minimize the distance between scan lines until it reach the value close to diameter of the atoms. Also the quality of images depends on the ability of the camera that determined the variation in the numbers of points which collected by the supplement of the device depend on the number of points per unit area that increase the quality of the images. It was observed that the time required to collect data is limited to less than (0.029)sec which depends on the speed of the scanner tunnel device.

Graphite topography

To interpret the image correctly, it must first be aware that bright spots show topographic high points and dark spots low ones. In the lattice model of graphite, line fit map and graph can be observed in figure 2-a and b. Also 3-Dimension view scan forward, shaded map forward, 3- Dimension view lateral and 3-Dimension view backward can be observed in figure 2(c),(d),(e) and (f) respectively. It can see that there are two different positions of carbon atoms in the graphite hexagonal crystal lattice. An atom with a neighboring in the plane below (gray) and one without a neighbor in the lattice below (white). As a consequence, the electrical conductivity of the graphite surface slightly varies locally, so that the atoms without neighbors appear higher (brighter) than the others. If the carbon atoms have direct neighbors in the layer below, these atoms will drag electron density from those above so they appear lower (darker). Black spots correspond with the space between surrounding carbon atoms of a C₆-ring, showing a minimum in the electron density of the surface. This layer structure causes the lattice constant between the bright “hills” to have the higher than normal value of 0.25 nm(value molecules from various literature is 0.246nm). STM is able to obtain images with nanometer resolution of molecules on metal surfaces. These high-resolution images reveal the molecular structure and arrangement of the molecules on the surface and contain information about the molecule – substrate interaction and the molecule – molecule interaction. These excited electrons can tunnel across the barrier. In other words, tunneling occurs mainly with electrons of energies near the Fermi level. However, tunneling requires an empty level that have of the same energy of the electron to enable it to tunnel into the other side of the barrier. According to this restriction, the tunneling current can be related to the density of the available filled states in the sample. The current due to the applied voltage V depends on two factors: 1) the number of electrons between E_f and eV in the sample, and 2) the number of free states have correspond to the tunnel into the other side of the barrier at the tip. The higher density of available states the greater the tunneling current. The exponential term in the above equations means that small variations in W greatly influence the tunnel current. If the separation distance is decreased by 1 Å, the current increases by the order of magnitude, and vice versa.^[22] If one found that he solved Schrödinger’s equation for each side of the junction separately to obtain the wave functions ψ and χ for each electrode, he could obtain the tunnel matrix, M , from the overlap of these two wave functions.^[51] This can be applied in STM by making the electrodes the tip and sample, assigning ψ and χ as sample and tip wave functions, respectively, and evaluating M at some surface S between the metal electrodes,

where $z=0$ at the sample surface and $z=W$ at the tip surface.^[51] The applying of filter will also decrease the resolution of the image. The electron cloud associated with metal atoms at a surface that extends in a very short distance above the surface. When a very sharp tip--in practice, a needle which has been treated so that a single atom projects from its end--is brought sufficiently close to such a surface, there is a strong interaction between the electron cloud on the surface and that of the tip atom, and an electric tunneling current flows when a small voltage is applied. The mean line per unit dimension as indicated in figure 2 (b), the positive part of the curve represents the atom position(white region), and negative part of the curve is the region between atoms(gray region). The cloud of electrons appears at the edge of the atoms that decrease in direction of separation region between atoms. It was noted that the dimension is (1.65nm) profile of images, which can be measured the radius of atoms by calculated number of atoms whose the value is equal to 0.13nm of (3 atoms +3 vacancies).

Gold topography

It is way more difficult to obtain good images of gold. Atomic structures are difficult to observe, because the electrons on the surface are much more homogeneously distributed than the graphite. The contrast on the image is due to variations in charge density.^[18] But, some training, the mono-atomic gold steps of topography, line fitting map and graph can be observed in figure 3(a) and (b). Also 3-Dimension view scan forward, shaded map forward, 3- Dimension view lateral and 3-Dimension view backward can be observed in figure 3(c),(d),(e) and (f) respectively. The multi-hills (white spots) that approach with each other to make tunneling by the electron in the potential barrier easy, hence the conductivity becomes high. The amorphousness in arrangement represents a depth stacking in gold atoms and overlapping in electronic clouds that appears as elliptical elongation because of the crowd of electron flux. The mean line graph of dimension indicated in figure 3(b), seems unsteady in position of atoms and is difficult to characterize the right position of each atom, in spite of the gold that is a good conductive material.

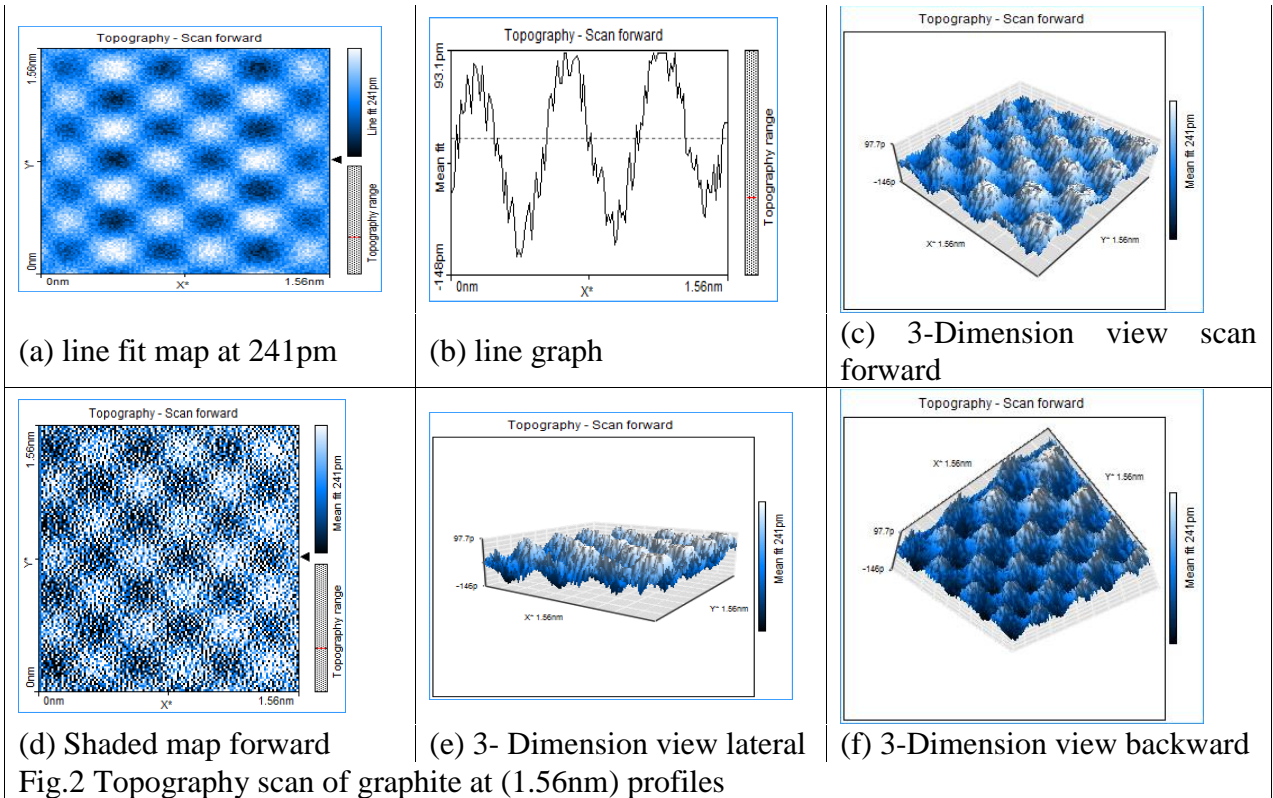
Silicon wafer (100) topography

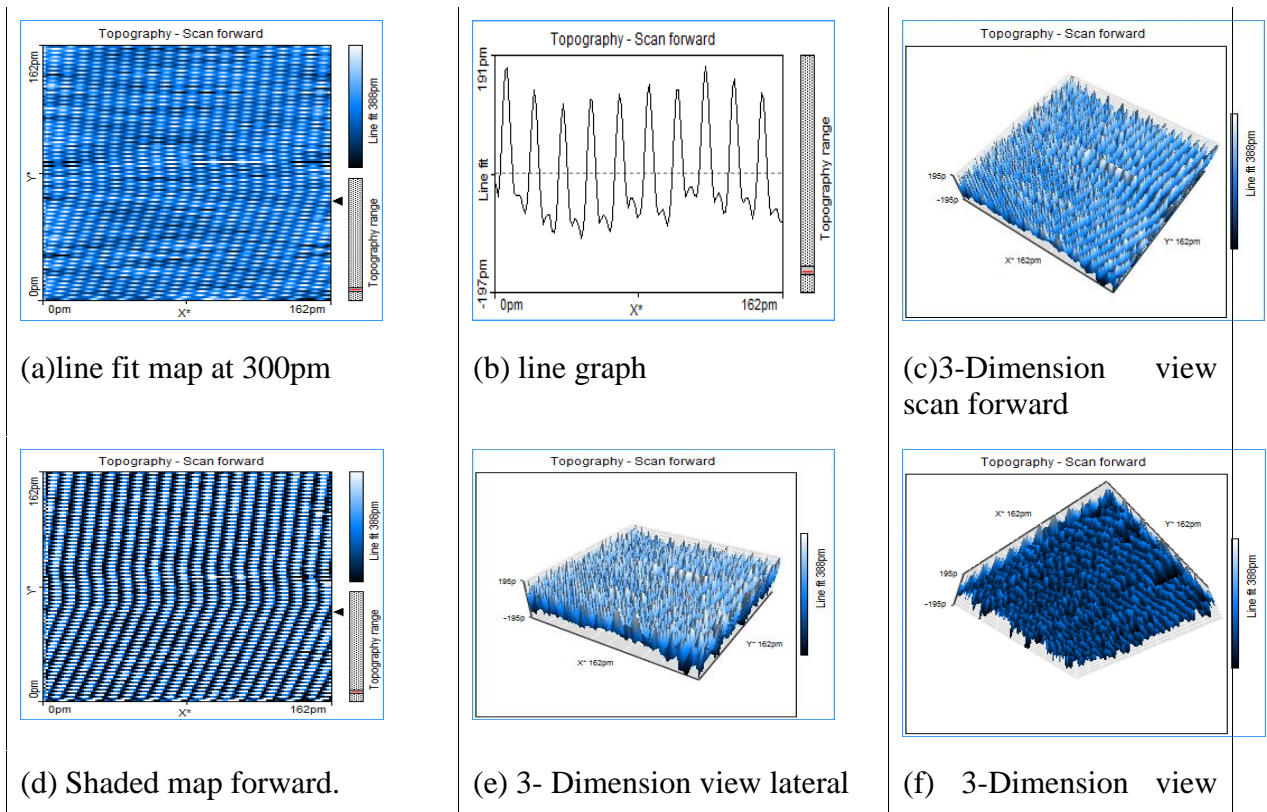
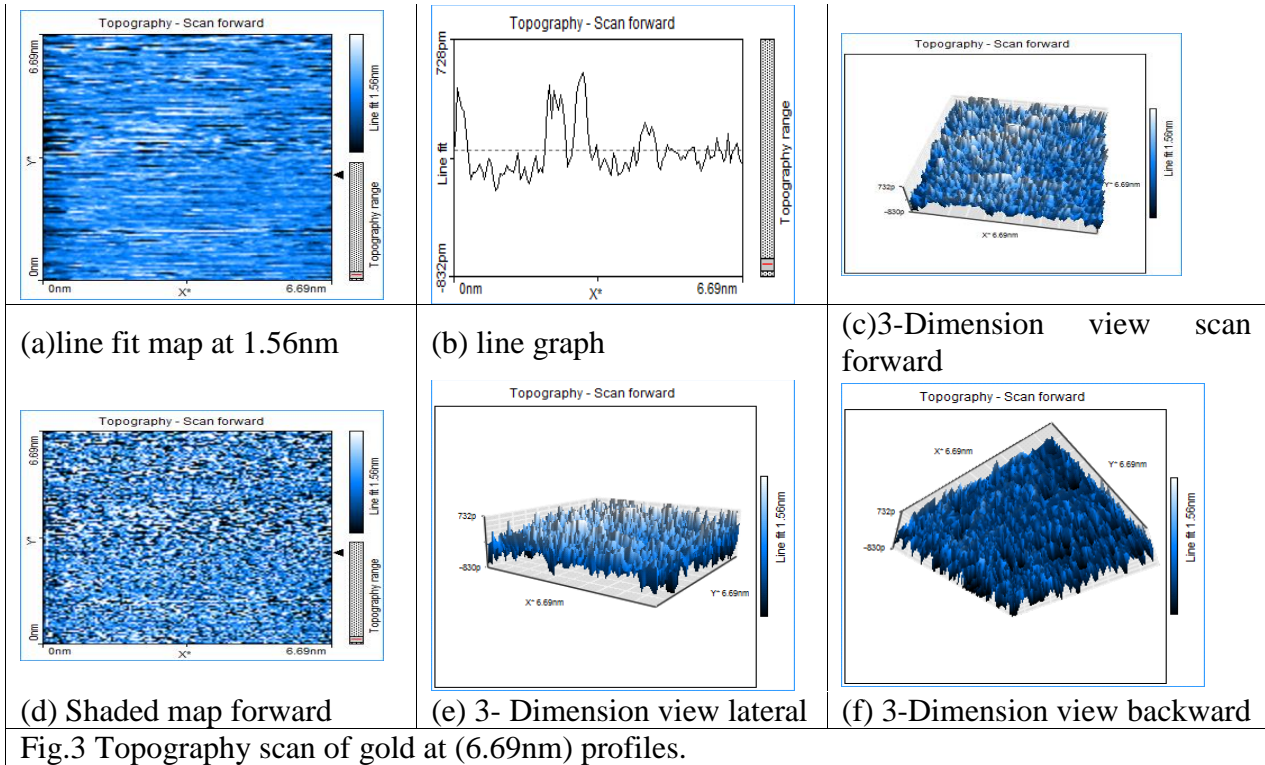
Three-dimensional representation of an scanning tunneling microscopy image of the silicon atoms at the edge of the silicon wafers of type pattern consist of bright, dark and brighter spots with very few numbers (doped silicon), and first be aware that bright spots show topographic high spots. An atom with neighboring atom in the plane below(dark)and without a neighboring in the lattice appears below(white) with tetragonal bonds. If silicon atoms in the row have linear defect (dislocation) that results from inserting extra atoms, the fit row line shown in figure 4(a). The deflection in the regular lattice sites, the graph can be observed in figure 2(b). Also 3-Dimension view scan forward, shaded map forward, 3- Dimension the lateral view structure refers to stacking row of atoms in y-line. and 3-Dimension view backward can be observed in figure 4-c,d, e and f respectively. The density of states at doped site can be compared with the density of states far from impurities. The line graph as shown in figure 4(b) contains positive parts that represent the atom positions(white spots), and the negative parts are the separation regions between atoms(dark spots). The gradient of the curve peaks means

there is a deflection of stacking atoms of silicon wafer (100). The number of atoms and vacancies are 20 with dimension of 162 pm and radius 0.405 nm in figure 4(a).

Cadmium oxide film topography

The surface morphologies of CdO films showed a grain growth with mixture of island-like and granular grain shapes. The grain boundaries (planer defects) tend to be loose bound. The Images of the polycrystalline structure of the film as shown in figure 5 (a,b,c,d,e,f), describes irregular positions of CdO molecules as a result of deposited film type . It consists of point defects (vacancy, self interstitial, extra atom, substitutional atom). So it is difficult to describe the aggregate of atoms in many positions. line fit map and graph line,3-Dimension view scan forward , shaded map forward , 3- Dimension view lateral and 3-Dimension view backward can be observed in figure 5a) and (b). (c),(e) and (f) respectively. The graph line against dimension also contains positive and negative parts of the curves depending on the position of atoms in the films. It is expected that the arrangements and positions of atom that described by images depend on preparation circumstances,(deposition rate, temperature, type of deposited material, ect.) as shown in figure 5(b). The form of aggregations is completed with calculation of evaluated grain size by X-ray.





backward

Fig.4 Topography scan of Si wafer (162pm) profiles

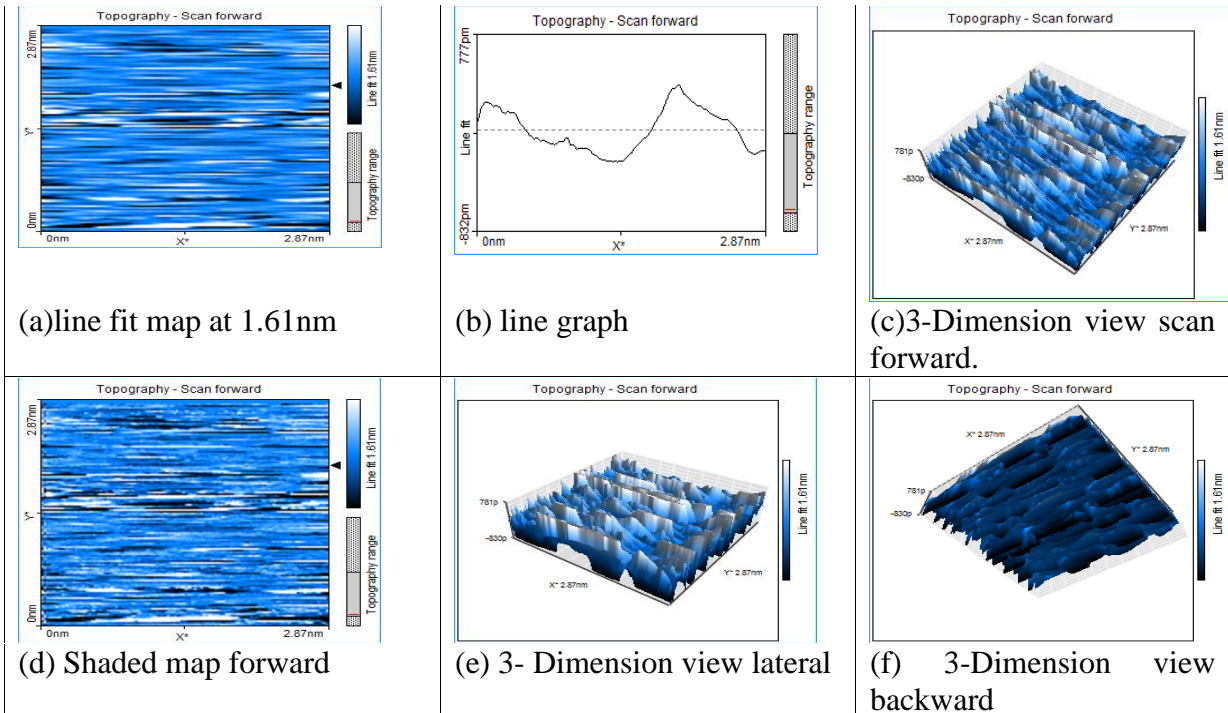


Fig.5 Topography scan of CdO film at (2.87nm) profiles

CONCLUSION

1- To be able to get such excellent pictures of atomic resolution is almost incredible the recent studies of electron confinement and quantum size effects on conductive (graphite, gold) and semi conductive (silicon, cadmium oxide) due to surfaces reports on progress in physics.

2- The topography properties can be described to dramatically reduce the defects of the crystal (conductors or semiconductors) and to realize critical parameters of the crystals from nano-dimensional.

3- The achieving nano-resolution for metals and semiconductors, Bandgap's nano-resolution processes are inexpensive, fast and controllable to be applied in technologies.

4- The used scanning tunneling microscope to validate first principle calculations - or models - that had predicted this outcome for years, and the formation mechanisms of new structures, determine the unit cells for complicated phases and the level of structural perfection.

5- The knowledge of specific nanoscale surface structures, periodic, random or pseudo-periodic, that led to agglomeration of metal clusters and to answer the old question

whether random or the periodic patterns is the best. This gives an important step to improve physics models.

REFERENCES

- Jannick Langfahl-Klabes.(2009).Phywe Series of Publications ,Scanning Tunneling Microscopy(STM) – Operating instruction and Experiments,1st Edition., *Systeme GmbH &Co.KG*. Germany.
- Binnig, G., Rohrer, H.. (1986).Scanning tunneling microscopy. *IBM Journal of Research and Development* 30: 4.
- MLA style: "Press Release: The (1986) Nobel Prize in Physics. Nobelprize.org. 16 Jun 2013.
- Bai, C. (2000). Scanning tunneling microscopy and its applications. New York: Springer Verlag.
- Julian, Chen C. (1993). Introduction to Scanning Tunneling Microscopy. Oxford University Press.
- Oura, K. Lifshits, V. G., Saranin A. A., Zotov A. V, and Katayama M. (2003). Surface science: an introduction. Berlin: Springer-Verlag.
- Carsten Sprodowski *et al*.(2010). *J. Phys.:* Condens. Matter 22 264005, Volume 22 Number 26.
- Wei-dong Dou and Han-jie Zhang. (2010). *Chin. J. Chem. Phys.* 23 18 Vol. 23 N 1.
- Hui-li Fan *et al*. (2010). *Chin. J. Chem. Phys.* 23 565,Vol. 23 N.5 .
- Flemming, Besenbacher. (1996). *Rep. Prog. Phys.* 59 1737 Vol. 59 N. 12.
- F M Leibsle *et al* .(1997). *J. Phys. D: Appl. Phys.* Vol.30.N 5 741,
- Schryvers, D. *et al* .(2013). *Sci. Technol. Adv. Mater.* Vol.14 N.1014206.
- Frank Palmino, Philippe Dumas, Frank Thibaudau, Philippe Mathiez, Christian Mouttet et Frank Salvan .(1990).Vol. 1, N.5-6, October / December ,pp 463 - 470.
- Terui, T. , Kamikado, T., Okuno, Y., Suzuki, H., Mashiko, S. (2004).,Nanotechnology Group, Kansai Advanced Research Center, *Communications Research Laboratory*, 588-2, Iwaoka, Nishi-ku, Kobe 651-2492, Japan. Vol. 4, Issues 2–4. April Pages 148–151.
- Zhang Yan-Feng , Gao Teng, Zhang-Yu, Liu Zhong-Fan .(2012).Controlled Growth of Graphene on Metal Substrates and STM Characterizations for Microscopic Morphology, *Acta Phys Chim Sin*,Vol.28, 2456-2464.
- Dixon, R. (2000).STM studies of semi conducting metal oxides, PhD Thesis, Oxford Univ., Condensed Matter. Vol. 588.*Materials Research Society*.
- Yamamoto, N. Kagami, S. Minoda, H, S. Kagami and H. Minoda, Dept. of Physics, Tokyo Institute of Technology, Meguro-ku, Tokyo 152–8551, Japan Vol. 588 - *Symposium P – Optical Microstructural Characterization of Semiconductors Editors*.
- Chambliss, D.D. ; IBM Research Division, Almaden Research Center, 650 Hany Road, San Jose, California 95120, USA ; Wilson, R.J. ; *Chiang, S. Journals & Magazines* Vol. 39 Issue:6.

- Bonnell, D. A. and Huey, B. D.. (2001). Basic principles of scanning probe microscopy. *Scanning probe microscopy and spectroscopy: Theory, techniques, and applications* (2 ed.). New York: Wiley-VCH.
- Pan, S. H.; Hudson, EW; Lang, KM; Eisaki, H; Uchida, S; Davis, J.C. (2000). Imaging the effects of individual zinc impurity atoms on superconductivity in $\text{Bi}_2\text{Sr}_2\text{CaCu}_2\text{O}_{8+\delta}$. *Nature* 403 (6771): 746–750.
- Schitter, G., Rost, M. J. (2008). Scanning probe microscopy at video-rate. *Materials Today* (UK: Elsevier) 11 (special issue): 40–48.
- Lapshin, R. V., Obyedkov, O. V. (1993). Fast-acting piezoactuator and digital feedback loop for scanning tunneling microscopes. *Review of Scientific Instruments* 64 (10): 2883–2887.
- Swartzentruber, B. S. (1996). "Direct measurement of surface diffusion using atom-tracking scanning tunneling microscopy". *Physical Review Letters* 76 (3): 459–462.
- STM carbon nanotube tips fabrication for critical dimension measurements. (2005). *Sensors and Actuators A: Physical*. 123-124: 655..
- Lapshin, R. V. (1995). Analytical model for the approximation of hysteresis loop and its application to the scanning tunneling microscope. *Review of Scientific Instruments* 66 (9): 4718–4730.
- Lapshin, R. V. (2007). Automatic drift elimination in probe microscope images based on techniques of counter-scanning and topography feature recognition. *Measurement Science and Technology* 18 (3): 907–927..
- Lapshin, R. V. (2004). Feature-oriented scanning methodology for probe microscopy and nanotechnology . *Nanotechnology* 15 (9): 1135–1151.
- Lapshin, R. V. (2011). Feature-oriented scanning probe microscopy.. *Encyclopedia of Nanoscience and Nanotechnology* 14. USA: American Scientific Publishers. pp. 105–115..
- Abelev, E; Sezin, N.; Ein-Eli, Y. . (2005). *Rev. of Sci. Inst*, 76..